DOI: 10.1002/anie.201406776

Calixarenes

Entrapment of Elusive Guests within Metal-Seamed Nanocapsules**

*Harshita Kumari, Ping Jin, Simon J. Teat, Charles L. Barnes, Scott J. Dalgarno, and Jerry L. Atwood**

Abstract: *Anions play a crucial role in locking alkali metals on the interior of metal–organic capsules that contain structural water gates. This role is further evidenced when stitching-up the capsule seam, resulting in either expulsion or trapping of cesium ions depending on the anion employed.*

The design of supramolecular complexes possessing transport properties is an exciting research area in biomimetic chemistry.[1] Significant advances have been made toward the controlled assembly of multicomponent nanometer-scale systems;[2] this has in part been undertaken with regard toward controlling guest encapsulation and the selective transport of ions. Molecular capsules, examples of this type of assembly, are capable of acting as hosts for adequately sized guest species.[3] The *C*-alkylresorcin[4]arenes and related *C*-alkylpyrogallol[4]arenes (general notation PgC_n) have been shown to form hexameric H-bonded capsules of ca. 10 Å radius (common capsule structure shown in Figure 1 A).[4] These assemblies have comparable internal volumes and their host–guest properties have been explored through various techniques including spectroscopy[3c,5] and small-angle neutron scattering (SANS).[2c,6]

The synthesis of discrete metal–organic supramolecular systems has seen major advances in recent years.[3d] In this regard a number of our studies have focused on the formation of metal-seamed hexameric PgC_n-based nanocapsules (for example, see Figure 1 B); these assemblies have dimensions and internal volumes akin to those of the H-bonded analogues, but structures can vary depending on the metal salts employed.[3d] Metal-seamed capsules of the general formula $[(\mathrm{PgC}_n)_6\mathrm{M}_{24}]$ result from reaction of PgC_ns with either $\mathrm{Cu^{II}}$ or $\mathrm{Ni^{II}}$ ions.[2c] This occurs by deprotonation of 48 PgC_n hydroxy groups (eight from each PgC_n subunit) and the metal–organic capsules conform to the near-spheroidal shape of their H-bonded analogues (Figure 1 A and B).[7] In contrast, reaction with $\mathrm{Ga^{III}}$ ions affords metal–organic capsules with the general formula $[(\mathrm{PgC}_n)_6\mathrm{Ga}_{12}]$ that possess water "gates" positioned distally within the hexameric assembly; this motif has a distorted "rugby-ball" shape in the solid state as shown in Figure 1 C.[8] Addition of $\mathrm{Cu^{II}}$ or $\mathrm{Zn^{II}}$ ions to preformed $[(\mathrm{PgC}_n)_6\mathrm{Ga}_{12}]$ capsules results in the formation of Ga/Zn and Ga/Cu mixed-metal $[(\mathrm{PgC}_n)_6\mathrm{M}_{24}]$ capsules by means of "stitching up" the capsule seam.[8,9] These mixed-metal capsules structurally adjust to afford near-spherical assemblies akin to that shown in Figure 1 B.[8,9] Notably, we have found that $[(\mathrm{PgC}_n)_6\mathrm{Cu}_{24}]$ and $[(\mathrm{PgC}_n)_6\mathrm{Ni}_{24}]$ are stable in solution, but that gallium-PgC_n assemblies structurally rearrange.[6c,2c] Recent experiments have shown 1) that $[(\mathrm{PgC}_n)_6\mathrm{Ga}_{12}]$ capsules rearrange from rugby-ball to toroidal geometry when dissolved in acetone[6c] and 2) that the mixed-metal $[(\mathrm{PgC}_4)_6\mathrm{Ga}_n\mathrm{Zn}_{24-n}]$ capsule also rearranges from spherical to toroidal geometry upon dissolution; the dimensions of this toroid differ from those found upon dissolution of $[(\mathrm{PgC}_n)_6\mathrm{Ga}_{12}]$.[6c] Such rearrangements are good examples of the self-assembly process wherein hydrogen bonds are reversible and can adapt to produce assemblies with a variety of shapes and sizes.

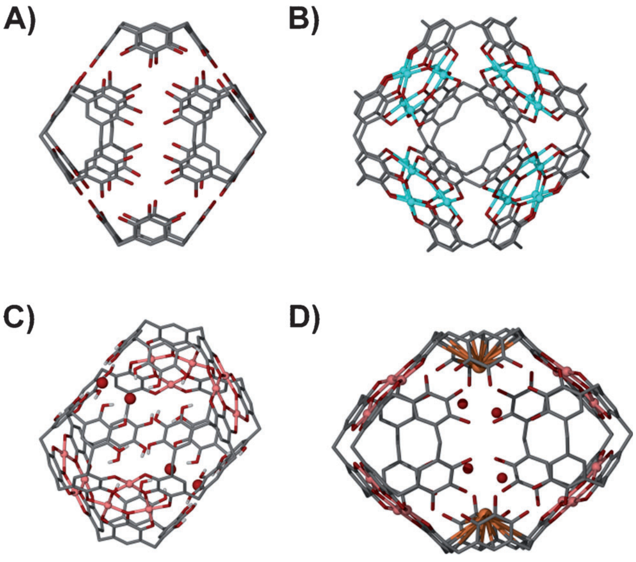

Figure 1. Hydrogen-bonded (A) and metal–organic (B–D) hexameric PgC_n nanocapsules. Color code: C grey, O red, Cu blue, Ga pink, H_2O red spheres, Cs orange. Hydrogens and lower rim PgC_n alkyl chains have been omitted for clarity. Figure is not to scale.

To gain insight into this critical problem, small-angle neutron scattering (SANS) data has been used to elucidate

---

[*] Dr. H. Kumari, Dr. P. Jin, Dr. C. L. Barnes, Prof. J. L. Atwood
Department of Chemistry, University of Missouri-Columbia
601 S. College Avenue, Columbia, MO 65211 (USA)
E-mail: atwoodj@missouri.edu
Dr. S. J. Dalgarno
Institute of Chemical Sciences, William Perkin Building
Heriot-Watt University
Riccarton, Edinburgh, EH14 4AS (Scotland)
Dr. S. J. Teat
Advanced Light Source, Lawrence Berkeley National Laboratory
Berkeley CA, 94720 (USA)

[**] We thank the NSF (J.L.A.), NSF CHE-95-31247, and NIH 1S10RR11962-01 for financial support of this work. We also thank Dr. Wei G. Wycoff for NMR support and valuable discussions. The Advanced Light Source is supported by the Director, Office of Science, Office of Basic Energy Sciences, of the U.S. Department of Energy under Contract No. DE-AC02-05CH11231.

Supporting information for this article is available on the WWW under http://dx.doi.org/10.1002/anie.201406776.

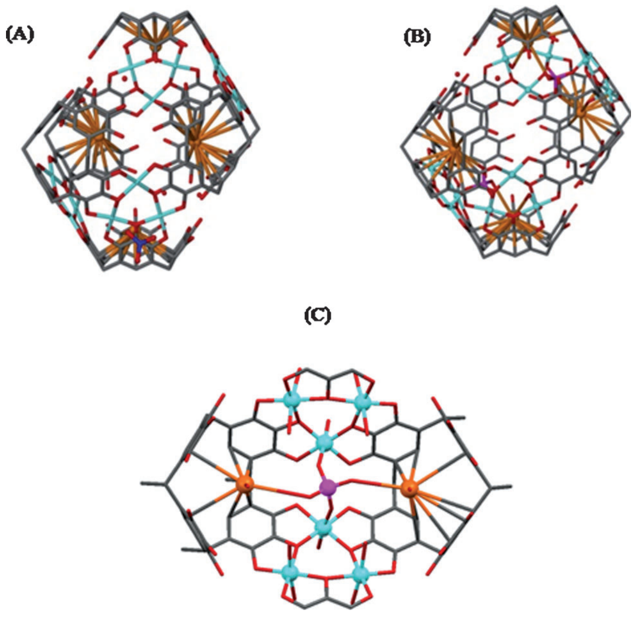

Figure 2. Single-crystal X-ray structures of the gallium metal–organic hexameric nanocapsules containing cesium interior ions synthesized from cesium nitrate (A) and cesium sulfate (B). C) Interaction of Cs with sulfate and one of the metal centers in the triad. Color code: C grey, O red, Ga blue, H_2O red spheres, Cs orange, N dark blue, S purple. Cs atoms are disordered and have partial occupancies. Hydrogen atoms and lower rim pyrogallol[4]arene alkyl chains have been omitted for clarity. Figure is not to scale.

the effect of temperature, solvent, and metal identity on the ratio of capsular products. Crystallization of these entities and their analysis by single-crystal X-ray diffraction (XRD) also served an important function in this study, not only in establishing the existence of both capsular species for the two metals investigated (Ni and Cu) but also as a method to verify purity. Although recrystallization of the hexameric moiety proved difficult, several reproducible methods have been developed for the isolation of crystalline Ni and Cu capsules of both the hexamers and their dimeric counterparts.

In 2008 we investigated the transport of silver nitrate or cesium hydroxide ion pairs across the water gates of $[(PgC_n)_6Ga_{12}]$ (Figure 1D).[8,10] Although ion transport across the capsule seam was achievable, our attempts to "stitch up" the assembly with a third metal (Zn) persistently resulted in Cs^+/Ag^+ expulsion.[10] We reasoned that guest expulsion could be attributable to 1) the choice of anion, 2) the toroid-to-toroid rearrangement in solution upon addition of Zn^{II} ions, and 3) the toroid-to-sphere rearrangement that occurs upon crystallization.[6c] As this was the case, we examined anion effects (nitrate and sulfate) in 1) controlling the expulsion of Cs guests across the water gates and 2) facilitating stitching of the capsule seam with a tertiary metal ion (Zn^{II}, K^I, or Rb^I). Here we show that modifying the Cs ion equilibrium in solution provides two novel routes to "lock" these on the capsule interior and that subsequent "stitching up" affords trimetallic PgC_n assemblies.

$[(PgC_4)_6Ga_{12}\subset CsNO_3]$ and $[(PgC_4)_6Ga_{12}\subset Cs_2SO_4]$ were formed by the addition of an excess of $MeCN/H_2O$ solutions of $CsNO_3$ or Cs_2SO_4 to preformed $[(PgC_n)_6Ga_{12}]$ in acetone. The solution containing $[(PgC_4)_6Ga_{12}\subset CsNO_3]$ remained clear during this process, but the $[(PgC_4)_6Ga_{12}\subset Cs_2SO_4]$ mixture was initially turbid, subsequently turning clear over time; to us this suggested a markedly different anion role in Cs entrapment upon moving from nitrate to sulfate. Slow evaporation of each clear solution led to the formation of single crystals that were suitable for X-ray diffraction studies. Based on the structural transformations observed for PgC_4Ga using SANS,[6c] it is evident from both structural analyses that $[(PgC_4)_6Ga_{12}\subset CsNO_3]$ and $[(PgC_4)_6Ga_{12}\subset Cs_2SO_4]$ must undergo "rugby-ball" to toroid to "rugby-ball" structural transitions upon dissolution and subsequent crystallization.

The asymmetric units in both $[(PgC_4)_6Ga_{12}\subset CsNO_3]$ and $[(PgC_4)_6Ga_{12}\subset Cs_2SO_4]$ comprise one half of a nanocapsule with three associated Cs ions that are present in different occupancies: interestingly only one Cs ion was located in the ASU for the previously reported $[(PgC_4)_6Ga_{12}\subset CsOH]$ nanocapsule. Elemental analyses of $[(PgC_4)_6Ga_{12}\subset CsNO_3]$ and $[(PgC_4)_6Ga_{12}\subset Cs_2SO_4]$ show Cs occupancies of 0.74 and 2.45 respectively. The higher Cs occupancy in $[(PgC_4)_6Ga_{12}\subset Cs_2SO_4]$ can be attributed to the aforementioned sulfate ions, which effectively anchor the Cs ions to the capsule wall (compare Figure 2A and B/C). Cs ions show polyaromatic interactions with the pyrogallol units of arene, similar to those observed in calixarenes.[11] Given that Zn^{II} ions were shown to stitch-up the structural water gates to form $[(PgC_4)_6Ga_nZn_{24-n}]$ mixed-metal nanocapsules,[9] we targeted this species with regard to investigating the permanent entrapment of Cs ions, utilizing either $[(PgC_4)_6Ga_{12}\subset CsNO_3]$ or $[(PgC_4)_6Ga_{12}\subset Cs_2SO_4]$ as starting materials. Addition of an ethanolic solution of excess $Zn(NO_3)_2$ to an acetone solution containing preformed $[(PgC_4)_6Ga_{12}\subset CsNO_3]$ resulted in expulsion of the enclosed Cs ions, as confirmed by XRD and scanning electron microscopy (SEM) elemental analyses. However, the integrity of the capsule in the solid state is maintained with the addition of zinc ions to the cesium-containing capsules. We believe that Cs expulsion can be attributed to 1) the position of the anion (in this case nitrate located on the capsule exterior), 2) rearrangement of the $[(PgC_4)_6Ga_{12}\subset Cs]$ toroid to the $[(PgC_4)_6Ga_nZn_{24-n}]$ toroid in solution, and 3) rearrangement of the solution-phase $[(PgC_4)_6Ga_nZn_{24-n}]$ toroid to spherical capsule in the solid state. Analogous addition of excess $Zn(NO_3)_2$ to $[(PgC_4)_6Ga_{12}\subset Cs_2SO_4]$ resulted in the successful entrapment of the Cs ions within the mixed-metal capsules, marking the first reported example of such a closed-seam trimetallic assembly (Figure 3). Elemental analysis of $[(PgC_4)_6Ga_nZn_{24-n}\subset Cs_2SO_4]$ reveals the presence of 1.5 Cs ions, whereas single-crystal X-ray diffraction confirms the presence of 1.7 Cs ions within the spherical mixed-metal capsule and these were found to be disordered over six positions, forming poly-hapto aromatic bonds with each of the PgC_4 subunits. Interestingly the Cs ion is retained upon stitching-up the $[(PgC_4)_6Ga_{12}\subset Cs_2SO_4]$ capsule seam (with $Zn(NO_3)_2$), with simultaneous loss of sulfate ions also occurring as confirmed by elemental and single-crystal XRD analysis. From these structural studies/alterations it is clear that the sulfate anion in case of Cs_2SO_4 plays an

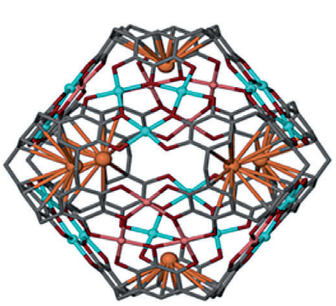

Figure 3. Single-crystal X-ray structure of the mixed Ga/Zn metal–organic hexameric nanocapsule with Cs ions permanently entrapped. Color code: C grey, O red, Zn blue, Ga pink, Cs orange. Cs atoms are disordered and have partial occupancies. Hydrogen atoms and lower rim pyrogallol[4]arene alkyl chains have been omitted for clarity.

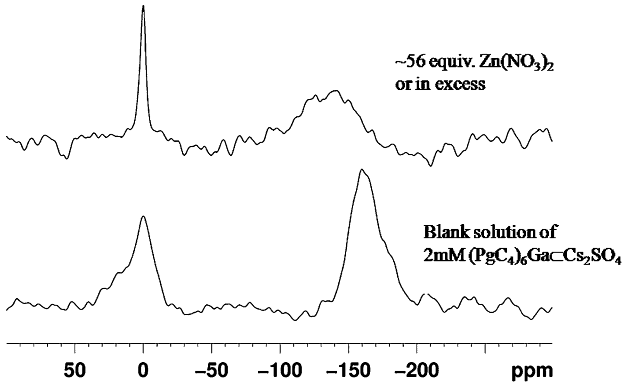

Figure 5. ^{133}Cs NMR spectra of $[(PgC_4)_6Ga_{12}\subset Cs_2SO_4]$ upon titration with ethanolic zinc(II) nitrate.

important role in anchoring the Cs ions within the capsule, shifting the relevant equilibria and thus promoting Cs encapsulation upon stitching-up the capsule seam.

To further investigate Cs entrapment we performed ^{133}Cs NMR experiments on $[(PgC_4)_6Ga_{12}\subset CsNO_3]$ and $[(PgC_4)_6Ga_{12}\subset Cs_2SO_4]$ with titration of ethanolic zinc(II) nitrate. The solid-state ^{133}Cs NMR spectrum of $[(PgC_4)_6Ga_{12}\subset CsNO_3]$ shows a peak at -160 ppm representing encapsulated Cs ions. These single crystals were then dissolved in [D$_6$]acetone to investigate the fate of Cs ions upon shifting from the solid state (rugby-ball) to solution phase (toroid).[6c] The resulting ^{133}Cs NMR spectrum shows peaks at 0 and -160 ppm representing both free and bound Cs ions, respectively (Figure 4). The two peaks suggest that a chemical equilibrium of Cs ions exists between the exterior and interior of the nanocapsule. Titration of ethanolic zinc(II) nitrate to this solution results in a marked reduction of the signal at -160 ppm, indicating expulsion of Cs ions from the assembly. Similar analysis of $[(PgC_4)_6Ga_{12}\subset Cs_2SO_4]$ in [D$_6$]acetone also reveals peaks at 0 and -160 ppm, and although this is the case, the area under the peak of encapsulated Cs is significantly greater than that of free Cs (Figure 5). This is consistent with the higher occupancy found in the solid state when sulfate (rather than nitrate) is employed as the Cs counterion. Addition of excess ethanolic zinc(II) to the solution results in both broadening of the peak at -160 ppm peak and sharpening of the peak at 0 ppm. This is consistent with structural studies and thus indicates a shift in equilibrium as well as permanent entrapment of some Cs ions on the nanocapsule interior. Notably, retention of the Cs ions occurs during rearrangement from solid-state rugby-ball→solution-phase toroid→solution-phase toroid→solid-state sphere. Drawing an analogy between SANS and NMR data suggests that the Cs is bound sufficiently well with the aid of the sulfate anion to affect its retention upon addition of zinc and stitching-up of the capsule seam. The structural rearrangement also accounts for the reduction in gallium ions from rugby-ball (12 Ga in $[(PgC_4)_6Ga_{12}]$) to spherical (12.5 Zn/11.5 Ga in $[(PgC_4)_6Ga_nZn_{24-n}]$) architecture in the solid state.[8] We can thus conclude that, in comparison to nitrate, the sulfate anion is shown to work as an inner force to not only anchor the Cs ions within PgC$_4$Ga, but also retain the target Cs ions during a structural shift induced by the addition of excess Zn^{II}.

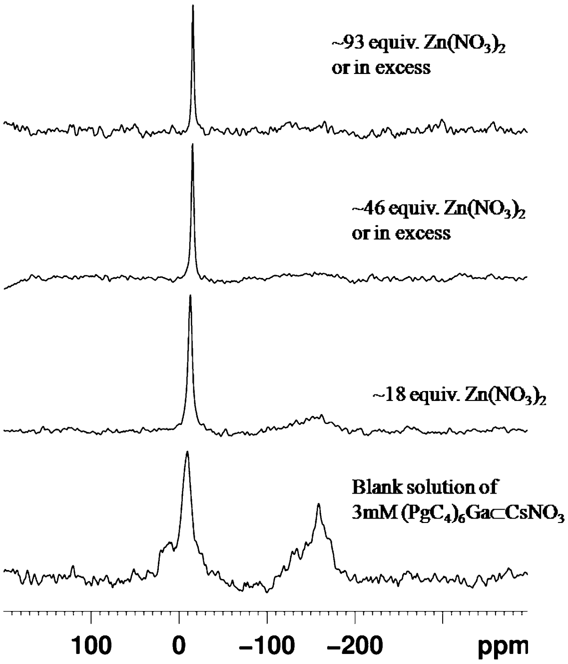

Figure 4. ^{133}Cs NMR spectra of $[(PgC_4)_6Ga_{12}\subset CsNO_3]$ upon titration with ethanolic zinc(II) nitrate.

Inspired by internal anion effects over capsule occupancy, we sought to employ external forces to promote Cs entrapment for both nitrate and sulfate counterions. For this purpose we investigated K and Rb as "fillers" for the structural water gates to facilitate Cs entrapment within $[(PgC_4)_6Ga_nZn_{24-n}]$, irrespective of the anion (nitrate or sulfate) employed. Literature indicates that potassium ions display weak cation–π interactions, but also that they can coordinate to upper-rim hydroxy O atoms of PgC$_n$s.[12] Addition of potassium nitrate in acetonitrile/water (v/v = 10:1) to an acetone solution of preformed $[(PgC_4)_6Ga_{12}]$ afforded single crystals upon slow evaporation. Single-crystal X-ray diffraction studies and elemental analysis confirm the presence of potassium ions as replacement for water in the structural gates of the nanocapsule (compare Figures 1C and 6). Each K^{I} ion is

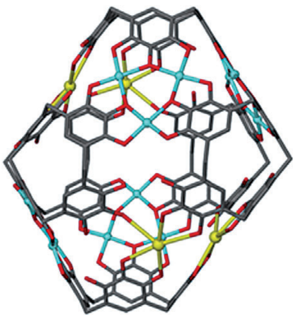

Figure 6. Single-crystal X-ray structure of the mixed Ga/K metal–organic hexameric nanocapsule. Color code: C grey, O red, Ga blue, K yellow. Hydrogen atoms and lower rim pyrogallol[4]arene alkyl chains omitted for clarity.

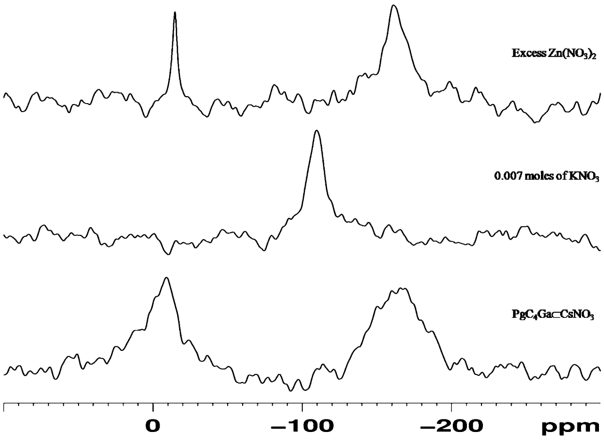

Figure 7. ^{133}Cs NMR spectra of [(PgC$_4$)$_6$Ga$_{12}$⊂CsNO$_3$] upon initial addition of excess potassium nitrate and subsequent addition of excess zinc nitrate.

coordinated to four equatorial hydroxy groups from two adjacent PgC$_4$s as well as two axial water molecules.

Titration of potassium nitrate in acetonitrile/water into an acetone solution of preformed [(PgC$_4$)$_6$Ga$_{12}$⊂CsNO$_3$] results in a drastic shift of both bound (−160 ppm) and free (0 ppm) Cs signals in the ^{133}Cs NMR spectrum (Figure 7), producing a merged peak at ca. −100 ppm. This suggests complete entrapment of Cs ions within the nanocapsule, a phenomenon confirmed by the subsequent addition of excess ethanolic Zn^{II} ions, which induces a reverse shift in the equilibrium and reappearance of the peaks at 0 and −160 ppm. The potassium ions residing in the gates of the [(PgC$_4$)$_6$Ga$_{12}$] nanocapsule are thus expelled by the Zn^{II} ions and slow evaporation affords single crystals of the expected mixed-metal nanocapsules as confirmed by structure analysis. Although the Cs ions were difficult to locate in this case due to poor quality diffraction data, their permanent encapsulation is confirmed by both ^{133}Cs NMR and SEM elemental analyses. Again, these new structures represent the first examples of the trimetallic (Ga/Zn/Cs and Ga/K/Cs) PgC$_n$ nanostructures in both solution and the solid state. Rubidium ions were also found to be capable of occupying the structural gates of the [(PgC$_4$)$_6$Ga$_{12}$] nanocapsule to afford a bimetallic species akin to that shown in Figure 6 for potassium. In contrast to the aforementioned titration of [(PgC$_4$)$_6$Ga$_{12}$⊂CsNO$_3$] with potassium ions, analogous experiments with rubidium show different behavior. Upon addition of small amounts of Rb^{I} there is initial merging of free (0 ppm) and bound (−160 ppm) Cs to produce a peak at $\lesssim -100$ ppm, but there is a subsequent shift to 0 ppm in the ^{133}Cs NMR spectrum as the concentration is increased. Clearly, Rb ions initially enhance the entrapment of Cs ions within the nanocapsule until a threshold value is reached. Beyond this threshold the equilibrium appears to shift in the reverse direction, expelling the Cs ions from the assembly. The comparatively stronger cation–π interactions of Rb^{I} with the polyaromatic PgC$_4$ framework allows this species to act both as a gate keeper and as a guest within the nanocapsule. Although this is the case, it is clear that both Rb^{I} and K^{I} are able to act as external driving forces for enhanced Cs entrapment in this system.

As sulfate and nitrate reside on the interior and exterior of [(PgC$_4$)$_6$Ga$_{12}$] nanocapsules, respectively, the differences in their response to K^{I} and Rb^{I} addition were of interest. Addition of K^{I} ions to [(PgC$_4$)$_6$Ga$_{12}$⊂Cs$_2$SO$_4$] in solution drives cesium entrapment, but an excess causes an increase in the peak corresponding to free Cs at 0 ppm. One possible explanation is that the sulfates also anchor potassium ions on the nanocapsule interior, a process that occurs with concomitant expulsion of some Cs ions. Titration with rubidium nitrate was also found to enhance Cs entrapment and an increase in peak height for the signal at −160 ppm was observed. A greater threshold value for Cs expulsion was observed in this case which we attribute to the influence of *endo*-capsule sulfate. Subsequent addition of ethanolic Zn^{II} once the threshold has been passed indicates only a small percentage of Cs entrapment in the ^{133}Cs NMR spectrum.

Overall, combined solid- and solution-phase studies provide real insight into the fascinating structural (sphere/toroid/rugby ball) and ion-transport properties of these nanometer-scale molecular capsules, and pave the way for future work in this exciting area.

Received: July 3, 2014

Keywords: calixarenes · cesium · encapsulation · ion transport · supramolecular chemistry

---

[1] a) C. Arnal-Hérault, M. Michau, M. Barboiu, *J. Membr. Sci.* **2008**, *321*, 94–99; b) G. W. Gokel, *Chem. Commun.* **2000**, 1–9; c) G. W. Gokel, P. H. Schlesinger, N. K. Djedovic, R. Ferdani, E. C. Harder, J. Hu, W. M. Leevy, J. Pajewska, R. Pajewski, M. E. Weber, *Bioorg. Med. Chem.* **2004**, *12*, 1291–1304.

[2] a) R. G. Harrison, O. D. Fox, M. O. Meng, N. K. Dalley, L. J. Barbour, *Inorg. Chem.* **2002**, *41*, 838–843; b) V. Percec, C. H. Ahn, G. Ungar, D. J. P. Yeardley, M. Moller, S. S. Sheiko, *Nature* **1998**, *391*, 161–164; c) H. Kumari, A. V. Mossine, S. R. Kline, C. L. Dennis, D. A. Fowler, S. J. Teat, C. L. Barnes, C. A. Deakyne, J. L. Atwood, *Angew. Chem. Int. Ed.* **2012**, *51*, 1452–1454; *Angew. Chem.* **2012**, *124*, 1481–1483.

[3] a) P. Ballester, G. Gil-Ramirez, *Proc. Natl. Acad. Sci. USA* **2009**, *106*, 10455–10459; b) S. J. Dalgarno, D. B. Bassil, S. A. Tucker, J. L. Atwood, *Angew. Chem. Int. Ed.* **2006**, *45*, 7019–7022;

Angew. Chem. **2006**, *118*, 7177–7180; c) S. J. Dalgarno, N. P. Power, J. L. Atwood, *Coord. Chem. Rev.* **2008**, *252*, 825–841; d) S. J. Dalgarno, K. M. Claudio-Bosque, J. E. Warren, T. E. Glass, J. L. Atwood, *Chem. Commun.* **2008**, 1410–1412.

[4] a) J. L. Atwood, L. J. Barbour, A. Jerga, *Chem. Commun.* **2001**, 2376–2377; b) L. R. MacGillivray, J. L. Atwood, *Nature* **1997**, *389*, 469–472.

[5] a) D. B. Bassil, S. J. Dalgarno, G. W. Cave, J. L. Atwood, S. A. Tucker, *J. Phys. Chem. B* **2007**, *111*, 9088–9092; b) S. J. Dalgarno, S. A. Tucker, D. B. Bassil, J. L. Atwood, *Science* **2005**, *309*, 2037–2039.

[6] a) H. Kumari, S. R. Kline, N. J. Schuster, J. L. Atwood, *Chem. Commun.* **2011**, *47*, 12298; b) H. Kumari, S. R. Kline, N. J. Schuster, C. L. Barnes, J. L. Atwood, *J. Am. Chem. Soc.* **2011**, *133*, 18102–18105; c) H. Kumari, S. R. Kline, W. G. Wycoff, R. L. Paul, A. V. Mossine, C. A. Deakyne, J. L. Atwood, *Angew. Chem. Int. Ed.* **2012**, *51*, 5086–5091; *Angew. Chem.* **2012**, *124*, 5176–5181.

[7] R. M. McKinlay, G. W. V. Cave, J. L. Atwood, *Proc. Natl. Acad. Sci. USA* **2005**, *102*, 5944–5948.

[8] P. Jin, S. J. Dalgarno, J. L. Atwood, *Coord. Chem. Rev.* **2010**, *254*, 1760–1768.

[9] P. Jin, S. J. Dalgarno, J. E. Warren, S. J. Teat, J. L. Atwood, *Chem. Commun.* **2009**, 3348–3350.

[10] P. Jin, S. J. Dalgarno, C. Barnes, S. J. Teat, J. L. Atwood, *J. Am. Chem. Soc.* **2008**, *130*, 17262–17263.

[11] B. M. Furphy, J. M. Harrowfield, D. L. Kepert, B. W. Skelton, A. H. White, F. R. Wilner, *Inorg. Chem.* **2005**, *44*, 4231–4236.

[12] B. F. Abrahams, N. J. FitzGerald, T. A. Hudson, R. Robson, T. Waters, *Angew. Chem. Int. Ed.* **2009**, *48*, 3129–3132; *Angew. Chem.* **2009**, *121*, 3175–3178.